Batteries & Supercaps

Review
doi.org/10.1002/batt.202400505

Chemistry Europe
European Chemical Societies Publishing

www.batteries-supercaps.org

"Dead Lithium" Formation and Mitigation Strategies in Anode-Free Li-Metal Batteries

Mozaffar Abdollahifar*[a, b] and Andrea Paolella*[c]

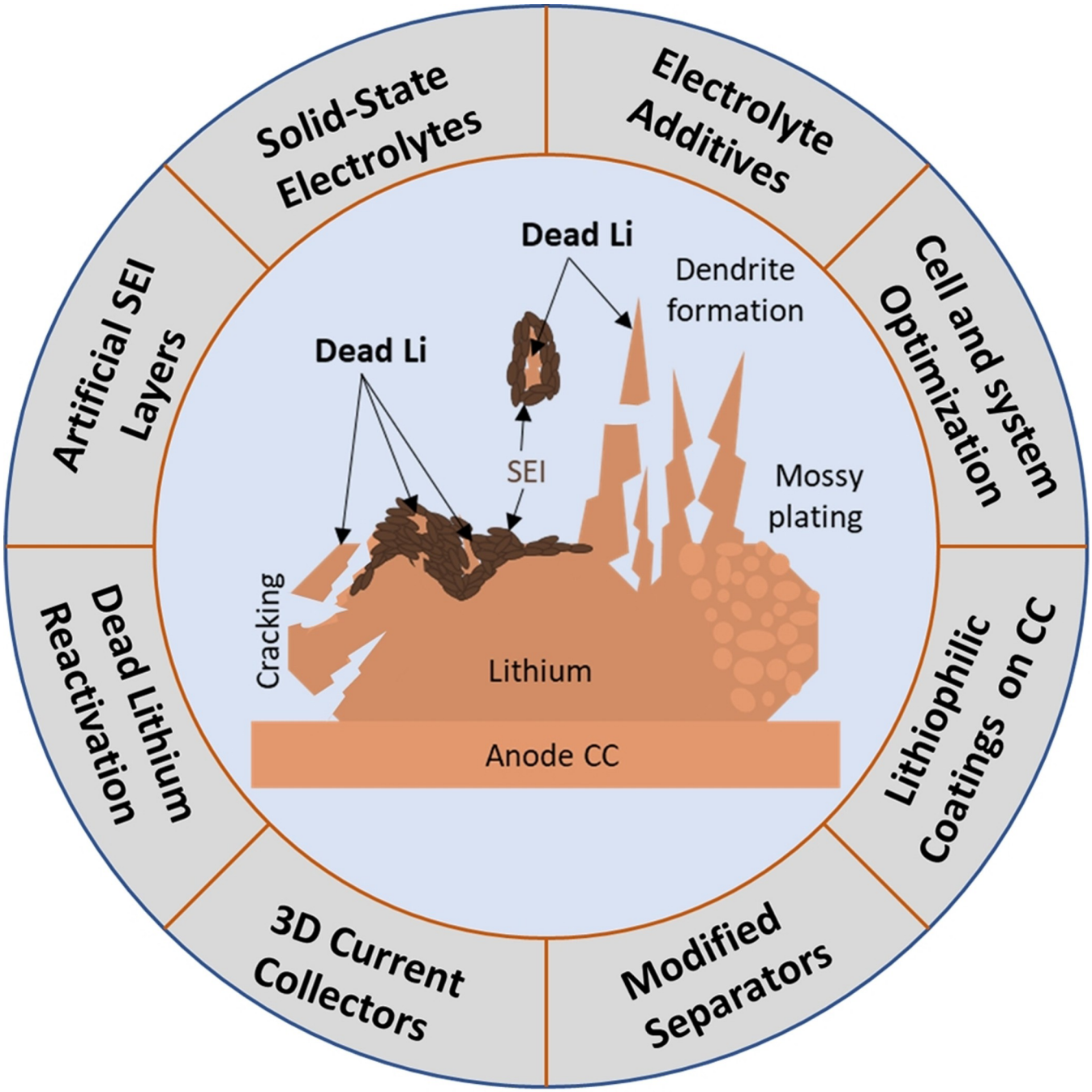

Thin lithium-metal foil is a promising anode material for next-generation batteries due to its high theoretical specific capacity and low negative potential. However, safety issues linked to dendrite growth, low-capacity retention, and short cycle life pose significant challenges. Also, it has excess energy that must be minimized in order to reduce the battery costs. To limit excess lithium, practical lithium metal batteries need a negative-to-positive electrode ratio as close to 1 : 1 as possible, which can be achieved through limiting excess lithium or using an "anode-free" metal battery design. However, both designs experience fast capacity fade due to the irreversible loss of active lithium in the cell, caused by the formation of the solid electrolyte interphase (SEI), dendrite formation and "dead lithium," – refers to lithium that has lost its electronic connection to the anode electrode or current collector. The presence of dead lithium in batteries negatively affects their capacity and lifespan, while also raising internal resistance and generating heat. Additionally, dead lithium encourages the growth of lithium dendrites, which poses significant safety hazards. Within this fundamental review, we thoroughly address the phenomenon of dead lithium formation, assessing its origins, implications on battery performance, and possible strategies for mitigation. The transition towards environmentally friendly and high-performance metal batteries could be accelerated by effectively tackling the challenge posed by dead lithium.

1. Introduction

Lithium metal foil is considered a promising anode to replace commercial graphite anode lithium-ion batteries (LIBs) due to its high theoretical capacity (3860 mAh g^{-1}) and lowest potential (−3.04 V vs standard hydrogen electrode).[1] Indeed, among lithium-metal batteries (LMBs) considerable attention has been drawn to the high capacities of lithium-air and lithium–sulfur batteries, which are achieved by utilizing lithium-metal as negative electrode.[2,3] lithium-metal foil is expensive: it's generally fabricated by electrolysis of lithium chloride (LiCl) component of the molten LiCl–KCl eutectic in the temperature range of 450–500 °C. The final lithium-metal ingot is rolled to produce 20 microns thick foil. Several advantages are associated with Anode-free LMBs (AFLMBs) technology:[4] (a) the use of metallic lithium anode can be eliminated reducing the fabrication costs related to the need of expensive lithium extraction;[5] (b) the in situ plating of thin lithium metal layer on CC as anode can effectively avoid safety risks associated with high content of lithium metal in a commercial battery cell;[6] (c) the preparation of AFLMBs doesn't require ultra-dry conditions unlike those needed when lithium metal is handled;[8] (d) AFLMBs can double the energy density of commercial LIBs to 500 Wh/kg and beyond[7,9,10] Moreover, in the future other alkaline and alkaline earth metals can be explored in order to furtherly reduce the battery costs (e.g Na, K, Mg, Ca).[4] However, AFLMBs face a significant challenge in lifespan, hindering practical applications. Minimizing irreversible loss of lithium and maintaining high Coulombic efficiency (CE) is crucial to achieve a long lifespan for metal batteries. Generally, LMBs can be cycled over thousands cycles[11] due to an excess of energy while AFLMBs has a limited cyclability. However, the development progresses have been impeded by safety concerns arising from dendritic lithium formation, repeated SEI formation and inactive, isolated or "dead" lithium formation during (dis)charge processes. Addressing safety concerns, dendrites play a significant role,[12] while the less formation of dead lithium improves the utilization of lithium during plating/stripping processes, thereby enhancing the cycle lifespan and CE of metal batteries. Strategies to prevent dendrite growth in lithium metal anodes include: optimizing the electrolyte for uniform lithium-ion flux distribution, designing lithiophilic lithium-matrix composites, using robust artificial SEI films, improving cycling efficiency, and regulating interfacial chemistry between the electrode and electrolyte.[13–15]

Disconnected isolated lithium fragments that lose electrical connection with the lithium electrode (anode) during stripping and are electrochemically inactive and electrically isolated by SEI are known as dead lithium. As cycling proceeds, dead lithium can consume the liquid electrolyte accumulating insulating species which accumulation can further block ion transport and lithium stripping, causing a self-accelerating positive feedback deterioration of batteries.[16] In the following sections, dead lithium formation and possible mitigation strategies will be discussed in details.

2. Dead Lithium

2.1. Dead Lithium Formation

About morphology, during cycling, a moss-like lithium deposit turns into a bulk lithium deposit, causing loose and porous lithium deposition and the accumulation of dead lithium. On the other hand, the dissolution of whiskers and needles with irregular and thin morphologies at the roots during cycling results in the formation of dead lithium. Electrochemically an irreversible loss of lithium-ions leads to decreased charge/discharge efficiency, resulting in lower energy conversion rates and increased heat generation. Therefore, dead lithium contrib-

[a] M. Abdollahifar
Chair for Functional Nanomaterials, Department of Materials Science, Faculty of Engineering, Kiel University, Kaiserstraße 2, D-24143 Kiel, Germany
E-mail: moza@tf.uni-kiel.de
[b] M. Abdollahifar
Kiel Nano, Surface and Interface Science KiNSIS, Kiel University, Germany
[c] A. Paolella
Department of Chemical and Geological Sciences, University of Modena and Reggio Emilia, Via Campi 103, 41125 Modena, Italy
E-mail: Andrea.paolella@unimore.it

utes to a gradual decrease in the battery's capacity over cycling, diminishing its energy storage capabilities. Dead lithium can also exacerbate safety concerns by promoting dendrite growth, internal short circuits, and thermal runaway events, posing risks of explosion. Figure 1a illustrates the mechanisms of dead lithium formation trapped inside SEI, through cracking and at the terminations of dendrites that have formed. These phenomena will be further discussed in the subsequent sections.

Yoon et al.[17] studied the formation of dead lithium by continuum mechanics model, and compared it with experimental results. They demonstrated that the dead lithium formation can easily be achieved by slowly stripping lithium deposits with irregular shapes, which often form after deposition at a fast rate (Figure 1b). This finding implies that in a battery, using a different (dis)charge rates within a cycle would pose a higher risk for forming dead lithium.

The formation of dead lithium has been investigated through the use of computational methods, for instance, mechano-electrochemical phase-field model,[18,19] continuum mechanics model.[17] Forming dead lithium was analyzed by Tewari et al.[20] through the use of a mesoscale computational model. They demonstrated that a higher temperature and lower overpotential lead to the formation of more dead lithium. By adjusting the overpotential, the rate of oxidation reactions can be influenced, while changing the temperature can have an impact on the diffusion kinetics of ions and lithium self-diffusion. The dead lithium formation depends more on self-diffusion of lithium at the solid interface than ionic diffusion.

Lee et al.[21] also simulated the dead lithium formation using reactive molecular dynamics (MD) studies. The growth of dead lithium and dendrite during repeated charging-discharging cycles can be seen in Figure 1c. At 20th–30th cycles, the dead lithium was formed with a sharp, thin, and fiber-like morphology. Shen et al.[18] simulates lithium stripping with both SEI rupture and stress-induced equilibrium potential shift in lithium batteries by mechano-electrochemical phase-field model. They demonstrated that external pressure during constant stripping current density can cause dead lithium formation, which can be prevented by electrolytes with high electrolyte elastic modulus and vertically aligned electrodeposited morphology. A probability-based mechanistic study by Tewari et al.[22] indicated that dead lithium formation is most likely when surface diffusion is higher during the stripping process. The phase field theory quantitatively calculates CE by linking the polarization curve and capacity loss peak.[19] Huang group[23] demonstrated that at low temperature of −20 °C, dendritic lithium have severe dead lithium production because of the preferential stripping at the root or kinked region. However, at higher temperatures of 25 and 60 °C, less discarded SEI and dead lithium existed owing to the compact deposition morphology. Therefore, minimizing the formation of dead lithium requires moderate reactivity of SEI-forming reactions and compact lithium deposition patterns.

A mechanism for dead lithium formation by Sanchez et al.[24] proposed (Figure 2a), and can be discussed as follows: dendrites nucleate near surface grain boundaries and within existing pits. New pits rarely form after the first cycle, and dendrites continue to nucleate inside the existing pits. As the pits grow larger, new surface area becomes available for subsequent dendrite nucleation. The initial planar electrode surface covered by a heterogeneous SEI experiences localized pit formation when an anodic potential is applied. Dendrites nucleate inside the pits and grow into large mossy structures. This process leads to a compact and tortuous dead lithium interphase, impacting mass transport through the electrolyte during extended cycling.

Sanchez and Dasgupta[25] suggested another mechanism as illustrated in Figure 2b. The concurrent nucleation of metallic lithium and SEI formation can be observed upon applying a charging current. This phenomenon has the potential to manifest on both the CC's surface and on the surface of the newly plated lithium. This process often leads to nonplanar morphologies and SEI fractures, exposing fresh lithium and causing dendritic growth. During discharge, inhomogeneous lithium stripping results in dead lithium formation. Dead lithium formation, indicated by increased cell polarization, creates surface pits that affect subsequent nucleation and growth. These pits, varying between liquid and solid-state systems, further complicate the battery's performance and longevity.

Additionally, the following are also could be summarized regarding the formation dead lithium in LMBs:

- More dead lithium is formed during stripping with diminution in current and increasing in temperature, as well as in thin and narrow interfaces.[23,26]
- Dead lithium formation caused by the dendrites lead to an increase of internal resistance.
- Additionally, lithium is more likely to form dead when diffusive processes are facilitated, rather than when oxidative reactions happen at the interface.[20]

Dr. Mozaffar Abdollahifar received his doctorate focused on energy storage materials from the National Taiwan University (NTU) in 2018. Before becoming a battery group leader at Kiel University, he worked as a scientist for several years at NTU and then at the Battery LabFactory Braunschweig (BLB, TU BS, Germany). He is interested in developing supercapacitors and battery materials for Li, Na and sulfur chemistries, anode-free batteries, electrode engineering, as well as recycling end-of-life batteries.

Prof. Andrea Paolella (Reggio Emilia-Italy, 1984) is an Italian-Canadian electrochemist and material scientist. He explored the synthesis of various nano- and micron-sized ceramic materials, such as oxide solid electrolytes (e.g, garnet LLZO, and NASICON LAGP) and positive electrodes (LiFePO4 or high voltage NMC). He is currently an Associate Professor of Inorganic Chemistry at University of Modena and Reggio Emilia (Modena, Italy). His research focuses on anode-less technology.

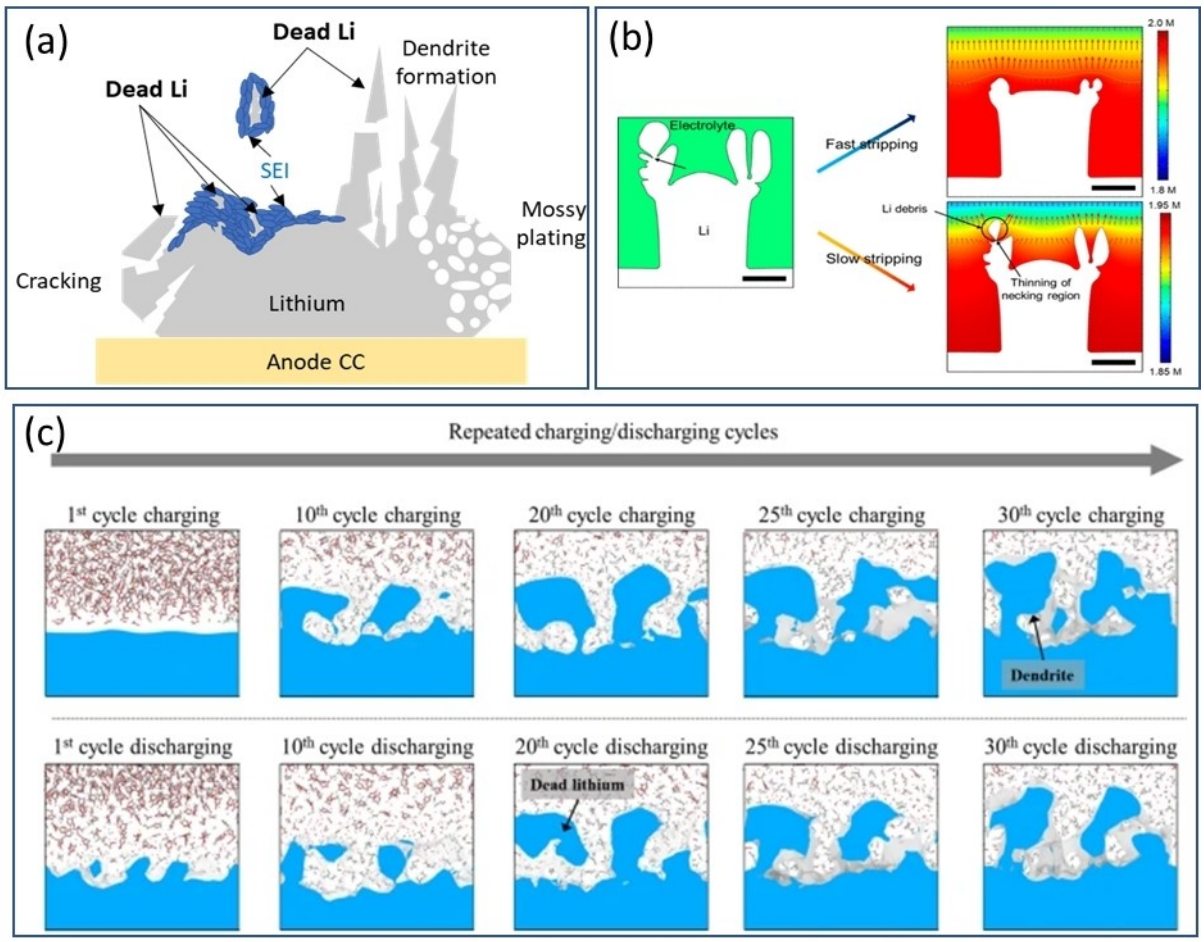

Figure 1. (a) Mechanisms of dead lithium formation. Dead lithium formation based on the simulation studies in LMBs: (b) A stripping behavior of lithium from an irregular deposit. For the slow stripping, dead lithium formation can be seen. The scale bars are 1 μm long. Reprinted with permission.[17] Copyright 2018, American Chemical Society. (c) Dead lithium and dendrite growth in response to repeated charges and discharges in pure EC electrolyte. Reprinted with permission.[21] Copyright 2022, Nature Publishing Group.

- Lithium loss could be dominated by the formation of dead lithium during cycling, whereas lithium loss due to interphase formation process (SEI and galvanic corrosion process) is much slower.[16]
- Dead lithium formation reduces surface area and increases overpotential and polarization.[19]
- Lithium plating morphology influences the formation of dead lithium. The formation of dead lithium deposits is less likely in nodule-like or sphere-like Li deposits compared to dendritic lithium deposits with high aspect ratios.[27–29]
- The presence of dead lithium on the lithiophilic sites in a 3D host obstructs the diffusion channels for lithium ions, leading to a failure in reducing the overpotentials required for nucleation.[30]

Dead lithium formation in LIBs: The generation of dead lithium are not limited to LMBs. But also in LIBs, the anode (typically graphite) could also form dead lithium under fast-charging and over-charging conditions. Vikrant et al.[31] performed computational and experimental studies to understand the occurrence of lithium plating and measure the amount of dead lithium on graphite electrodes. They demonstrated that dead lithium was observed for SOC over 60% and C-rates ranging from 4 C to 6 C. However, there was no dead lithium observed for SOC below 60% and low C-rates. The $LiNiCoAlO_2$ cathode enriched with Al on the surface can also effectively suppressing the oxidative decomposition of the electrolyte, gas generation, and dead lithium formation on graphite anode.[32] A physics-based model was presented by Duan et al.[33] based on a detailed description of graphite active particles to describe the lithium deposition-stripping process and particularly the formation of dead lithium.

2.2. Structural and Chemical Characterizations of Dead Lithium

As reported by Zhu et al.[34] it's possible to follow the dead lithium formation along 110 facet by in situ X-Ray diffraction (XRD): the authors modified a standard 2032 coin cell using a 5-micron thick copper as a CC. The presence of dead lithium was observed as residual lithium at the end of the discharge process as shown in Figure 3.

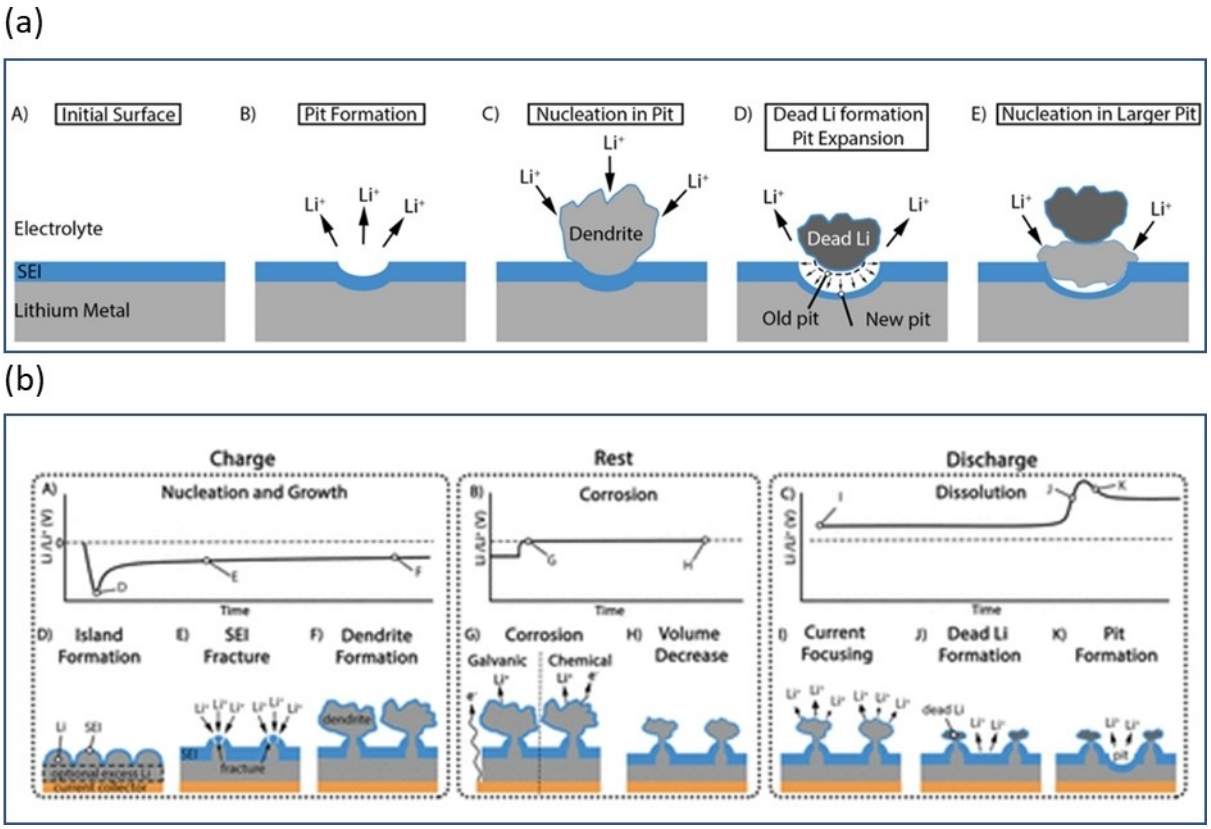

Figure 2. (a) lithium electrode with SEI before cycling, (B) lithium electrode after dissolution forming pits, (C) dendrite formation during deposition, nucleation inside pit, (D) dead lithium formation and pit expansion after dissolution, and (E) dendrite nucleation inside expanded pit, displacing dead lithium. Reprinted with permission.[24] Copyright 2020, American Chemical Society. (b) The process of lithium cycling can be delineated into three sequential phases. Reprinted with permission.[25] Copyright 2024, American Chemical Society.

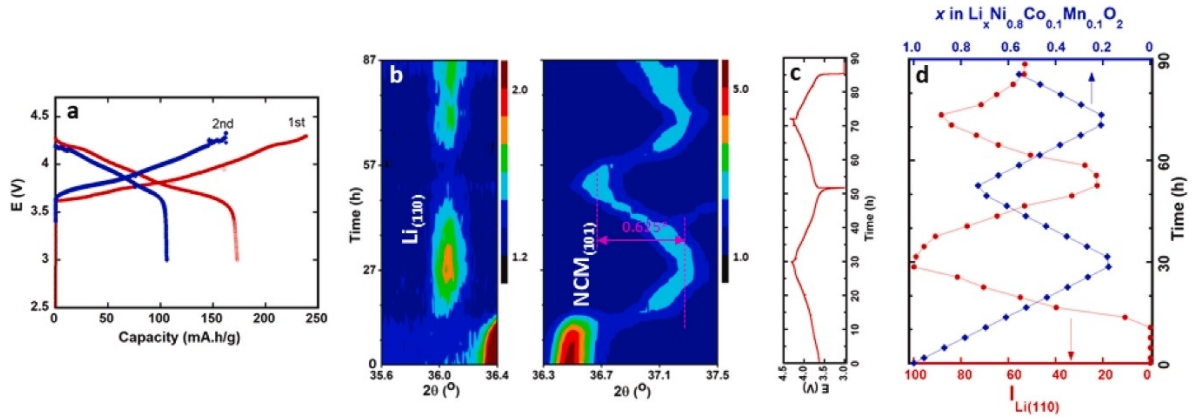

Figure 3. The electrolyte cell, containing LiTFSI-DME-TTE, underwent 2 cycles between 3.0 and 4.3 V at a C/24 rate, followed by a 4 hour CV = 3 V. (a) Capacity; (b) Evolution of lithium (110) and NCM (101) lines; (c) Voltage vs. time; (d) Variation of normalized lithium (110) intensity (red) and average lithium content (blue) in NCM. Reprinted with permission.[34] Copyright 2022, Elsevier.

Scanning electron microscope (SEM),[35,36] in situ environmental transmission electron microscopy (TEM),[37,38] n-situ electrochemical liquid TEM,[39] in situ/operando optical microscopy,[24,40–42] X-ray microtomography,[43] photoacoustic (PA) imaging for 3D visualization[16] and magnetic resonance imaging[44] are methods for give a morphological perspective without providing a chemical information. Metallic dead lithium and Li^+ in SEI can be differentiated by cryogenic TEM,[45,46] and X-ray photoelectron spectroscopy (XPS)[47] with a limited to surface or local area detection. Kourkoutis et al.[48] found two dendrites on the lithium anode using cryo-focused ion beam (cryo-FIB) and cryo-scanning transmission electron microscopy (cryo-STEM). The dendrite that mostly made of brittle LiH disconnects easily from the electrode and forming dead lithium.

However, quantitative methods such as titration gas chromatography[1,49] and in-situ nuclear magnetic resonance

(NMR) procedure[50] are effective in observing dead lithium formation.[51–53] Grey group demonstrated that in-situ NMR is a non-destructive method that can quantify dead lithium formation and formed microstructures during battery operation. The formation of dead lithium in AFLMBs was tracked using in situ ^{7}Li NMR, and the rate of corrosion of lithium metal during the open circuit was also studied.[54,55] Inhibiting the growth of dead lithium can be achieved easily and effectively by applying stacking pressure.[56,57] Lin et al.[58] used in NMR spectroscopy to study the effect of stacking pressure on dendritic behavior and dead lithium formation. The study found that low and high stacking pressures (0.1 and 1.0 MPa) leads to dendrites and dead lithium, while 0.5 MPa stacking pressure produces the least amount of dead lithium (Figure 4). The ^{7}Li NMR spectra for dead lithium indicated that dendrite lithium grows massively at low pressure, and production of mossy lithium occurs at high pressure.

Additionally, combination of gas chromatography (GC) and electrochemical cycling with impedance spectroscopy can also measure the lithium rates caused by formation of dead lithium.[16] Furthermore, lithium lost due to corrosion and dead lithium formation could be quantified by operating X-ray diffraction (XRD).[59]

Titration gas chromatography (TGC) could be utilized as a method to determine the quantity of the dead lithium.[60–63] Fang et al.[1] conducted experiments to measure the metallic Li^0 through TGC. Additionally, they used cryogenic electron microscopy to examine the microstructure and nanostructure of the unreacted metallic Li^0. The purpose was to understand the formation mechanism of dead lithium in different electrolytes and to identify the root cause of the low CE in lithium plating/stripping processes in LMBs. In addition, they proposed the following strategies to improve lithium plating/stripping efficiency: (i) To reduce unreacted Li^0 residue, lithium deposits should have a columnar microstructure with large grains and minimal tortuosity. (ii) The SEI should be chemically and spatially homogeneous, mechanically elastic, and refilled during cycles. Advanced electrolytes, artificial SEIs, and 3D hosts can help meet these requirements and provide a sturdy structural connection to guide lithium plating/stripping. In their study, they showcased using a 3D Cu foam to improve CE from 82% to 90%, surpassing the performance of 2D Cu CCs. This improvement can be attributed to the reduction in unreacted metallic Li^0. However, it is worth noting that the higher surface area of the 3D Cu foam resulted in an increase Li^+ from in SEI. Furthermore, their findings indicated that applying a pressure of around 5 psi induces structural collapse towards the CC, enhancing the structural connection and minimizing the formation of unreacted metallic Li^0.

The mass spectrometry titration (MST) technique can be used to differentiate between the presence of inactive lithium and lithium in SEI components.[64–66] Tao et al.[67] employed MST and NMR techniques to quantify the dead lithium formation with electrolyte optimization, and found that adding fluoroethylene carbonate (FEC) in the electrolytes mainly hinders the formation of dead lithium and LiH. They used deuterium-oxide (D_2O) to react with dead lithium and LiH for quantification measurements based on the according to the following reactions: $2Li + 2D_2O \rightarrow 2LiOD + D_2$, $LiH + D_2O \rightarrow LiOD + HD$. In another study, Daubinger et al.[68] also used FEC and high external pressure on the cells could reduce the formation of mossy and dead lithium and improve performance. Yang group[69] analyzed the impact of gas-producing reactions on the dead lithium formation using ethylene carbonate as a case study determined by MST method (Figure 5). Ethylene carbonate decomposition continuously releases ethylene gas, which reacts with lithium metal to form inactive species LiH[70] and Li_2C_2.[71] The presence of lithium carbide species was also detected at the interface between lithium metal and solid electrolyte (polymer[72] and ceramic[73]) in solid state batteries: these results demonstrate that its formation is independent of the physical state of the electrolyte used. Phase-field simulations showed that non-ionically conducting gaseous species could result in uneven Li-ion distribution, enhancing the

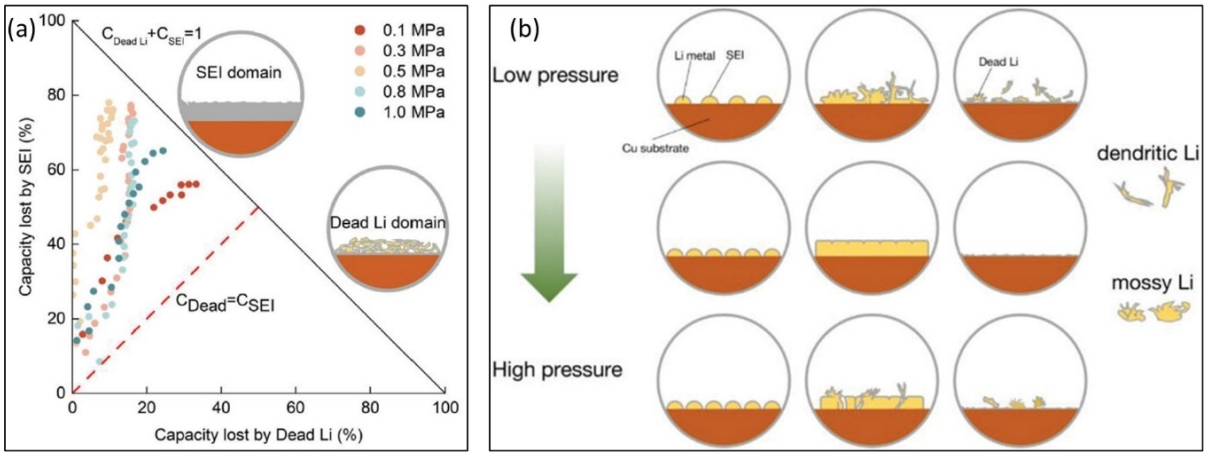

Figure 4. (a) Battery failure mode after plating at various stacking pressures for a AFLMB. (b) The diagram demonstrates stacking pressure influences on the lithium metal deposition and the dead lithium formation. At low stacking pressure, mossy and dendritic lithium metal forms, while high stacking pressure leads to planar deposits with potential cracks contributing to dendrite growth. Dead lithium production at moderate pressures is minimum. Reprinted with permission.[58] Copyright 2024, Wiley.

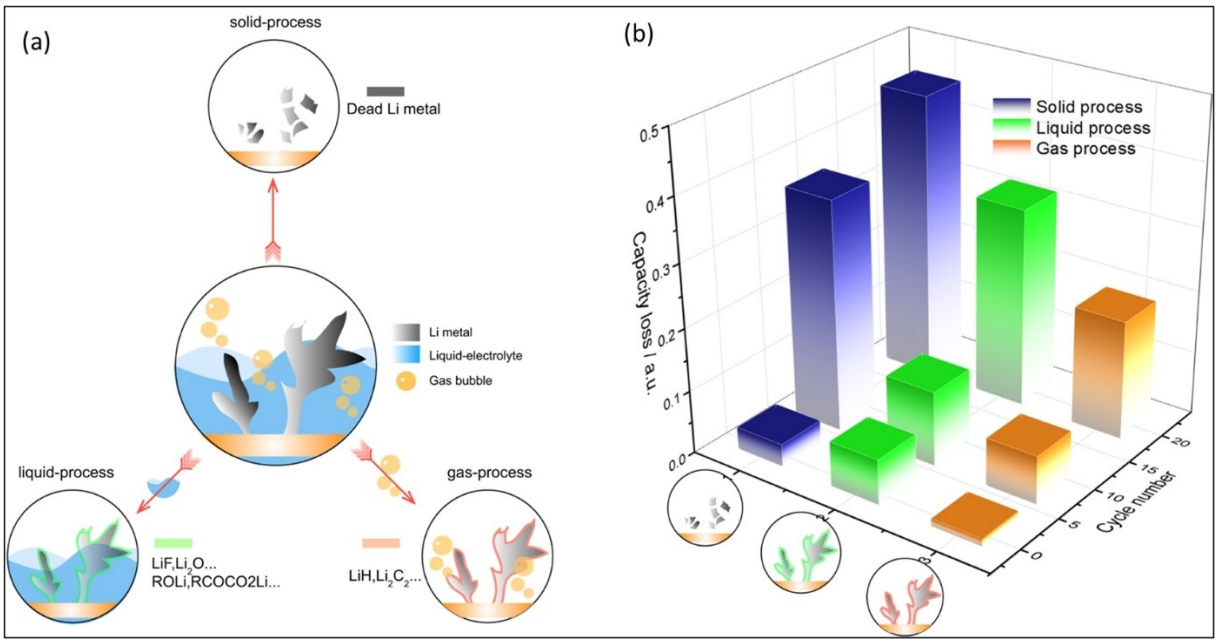

Figure 5. (a) Inactive lithium can be produced in three ways: (i) solid process, where it exists as dead lithium metal, (ii) liquid process, which involves reactions between the liquid electrolyte and lithium metal, and (iii) gas process, which occurs through reactions between gas species and lithium metal. (b) The assumption is made that inactive lithium in the baseline electrolyte is distributed in the following manner: (i) The chemical reaction between lithium metal and gas species leads to the formation of Li_2C_2 and LiH. (ii) The reaction between lithium metal and the liquid electrolyte accounts for the remaining inactive lithium (excluding dead lithium metal, LiH, and Li_2C_2). Reprinted with permission.[69] Copyright 2023, Nature Publishing Group.

formation of dendrites and dead lithium. Therefore, optimizing electrolyte composition to suppress ethylene gas formation is necessary.

Through the use of operando NMR, ex-situ TGC, and MST techniques, Xiang et al.[74] have established a method for quantifying the evolution of dead lithium and SEI. Through these three techniques, dead lithium metal can be quantified with deviations due to the presence of LiH. According to the unambiguous identification of LiH, the TGC method alone cannot accurately quantify dead lithium metal.

In addition to experimental analysis, theoretical and simulation studies involving COMSOL,[75,76] finite element method (FEM),[77] and molecular dynamics (MD)[21] are used to investigate the behavior of dead lithium, which is out of the scope of this paper and interested readers should refer to the references.

3. Mitigation Strategies

In order to improve the capacity retention of AFLMBs, two factors are crucial: (i) the extent reduction of SEI formation and (ii) the formation of dense lithium metal deposit. Dead lithium formation could be caused by faster stripping of lithium at sites with low impedance (thin and/or ruptured SEI layers). To address the challenges posed by dead lithium, various mitigation strategies can be explored trough optimizing the electrolyte chemistry,[78–81] interfacial properties,[82–84] electrode architecture,[85,86] implementing electrolyte additives,[87] separator,[88,89] and electrode designs as well as employing artificial SEI[90] to inhibit dendrite formation and reduce dead lithium. Several mitigation strategies have been thoroughly investigated and will be discussed in the following paragraphs.

3.1. Use of Additive

The formation of a SEI layer on the electrode surface during cycling can trap Li-ions, limiting their reversibility and contributing to dead lithium (Figure 6a). The formed SEI derived from carbonates reduction can be electronic insulator, creating dead lithium. This occurs when unreacted lithium is encased in a thick SEI layer but without electrical conductivity at the surface of anode electrodes.[14] Having a highly resistive SEI on lithium metal anodes leads to dead lithium formation, so it is important to target a high conductivity.[92] A flexible and stable SEI is key to reducing dendrite formation and dead lithium and improving the lithium metal anode capacity retention. Developing advanced electrolyte formulations and electrode coatings to enhance the stability and conductivity of the SEI layer, thereby reducing irreversible lithium trapping and dead lithium. For instance, electrolytes that result in fast SEI formation and homogeneous SEI coverage can help reduce dead lithium and stabilize capacity losses. An inorganic SEI layer with 3 d structure made of Li_2S and Li_3N on porous graphene oxide films prevents dendrite growth and dead lithium formation. It also improved Li-ion transfer and avoids lithium loss and electrolyte consumption seen with organic SEIs.[75] Zhu et al.[87] studied different electrolytes with salts like $LiPF_6$, LiDFOB, and LiFSI to understand lithium loss during cycling. Their findings show that SEI Li^+ and dead lithium accumulation contribute to lithium

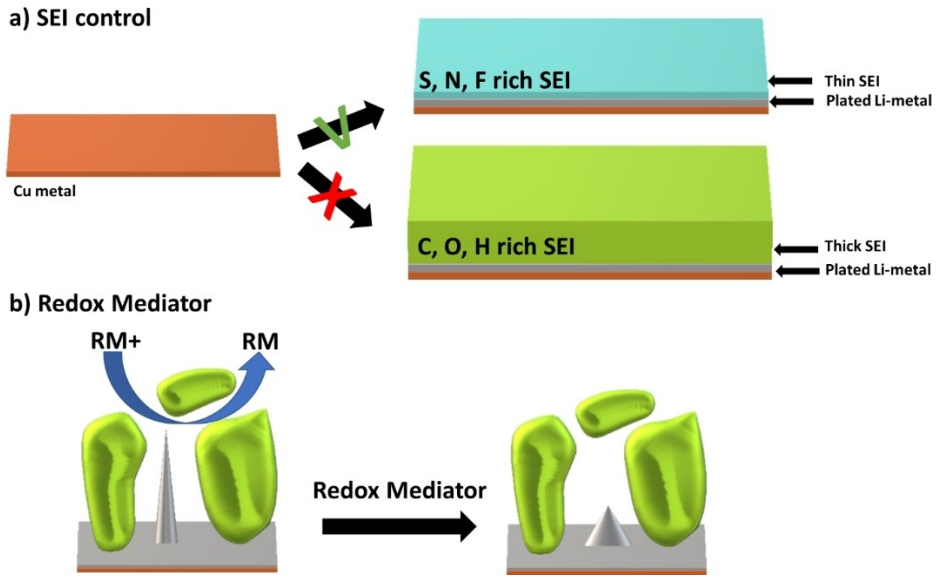

Figure 6. Schematic representing (a) the SEI control through the use of electrolyte additive and (b) the delithathion of dead lithium after reaction with a redox mediator.

loss with $LiPF_6$ salt, while dead lithium accumulation is the primary cause of lithium loss for LiDFOB and LiFSI salts. They also found that lithium nitrate and fluoroethylene carbonate additives can inhibit dead lithium and SEI Li^+. Recently, Zhang et al.[93] used 2-fluoro-5-iodopyridine, which contains a 2-fluoropyridine ring and an iodine atom in its structure, as an approach to forming a stable SEI, riched with LiF and Li_3N, and transforming dead lithium into active lithium by forming I_3^-/I^- ion pairs during the cycling process, resulted in longer and stable cycling life (Figure 6b). Stuckenberg et al.[94] studied the impact of adding $LiNO_3$ from a separator to carbonate electrolytes on lithium metal deposition and dead lithium formation in a NCM622||Cu cell. Consistently introducing $LiNO_3$ from separator resulted in a stable SEI on the anode electrodes, leading to improved capacity retention, enhanced CE, and the formation of dense lithium deposits.

Redox mediators with redox potentials between the cathode material's redox potential and the cut-off voltage of full cell could be employed for reactivating dead lithium and possess little self-discharge behaviors in AFLMBs.[95] For reclaiming inactive lithium, Jin et al. developed a reversible I_3^-/I^- redox couple initiated by SnI_4, which converts inactive lithium into soluble LiI, that moves to the cathode side. LiI is oxidized by a delithiated cathode, reclaiming Li-ion by lithiating the cathode and regenerating I_3^-. Additionally, Sn acted as a carrier of iodine and reduced extra corrosion of I_3^- on active lithium, improving the cyclability of LMBs.[79,96] Other redox mediators[97] have been tested as additive showing promising results such as TEMPO[98] and ferrocene.[91] In summary the use of additives to mitigate dead lithium formation is relatively easy and low cost although during cycling they may degrade losing effectiveness.

3.2. Modification of CCs

The anode experiences dendrite formation due to nonuniform lithium-ion flux, which leads to the accumulation of dead lithium caused by lithium stripping behaviors occurring at the dendrite tips or the nonuniform dissolution the dendrites may result in forming dead lithium (Figure 7). For example, Dasgupta group[24] demonstrated that a dead lithium's formation is influenced more by dendrite nucleation and pit formation than by growth. It has been shown that a dendritic morphology characterized by poor electrical contact with the CC leads to persistently high dead line growth, whereas a nodule-like morphology led to a more complete stripping method and a significantly reduced dead line growth rate.[23] A promising method to prevent dendrite growth and dead lithium formation is to use 3D CCs as frameworks for LMBs (Figure 7a). Using the combustion method, Peng et al.[76] fabricated a 3D structured zinc oxide-loaded Cu foam as a CC, resulting in uniform lithium deposition throughout the CC's interior, without dendrites or dead lithium residue in LMBs. Investigating novel electrode materials, and CC for AFLMBs,[99] with enhanced lithium diffusion kinetics and improved structural stability to mitigate side reactions that produce dead lithium. Qing et al. have developed a dendrite-free 3D composite lithium anode called Li–B@SSM. It has a high CE of 99.95% and a long lifespan of 900 hours. The anode reduces lithium dendrites, dead lithium accumulation, and volume changes through site-selective plating behavior and spatial confinement effect.[100] The use a lithiophilic layer (Ag, Zn, Mg, Al) can promote a homogenous lithium metallic layer (Figure 7b): Azfali et al.[101] have demonstrated that a Zn@Cu anode could maintain the CE above 90% for 290 cycles at 1 mA/cm^2 in asymmetrical Zn@Cu//Li cells. Shin et al.[102] have prepared an Ag@Cu electrode by cation exchange reaction. During the first charge the alloy $Li_{20}Ag$ is

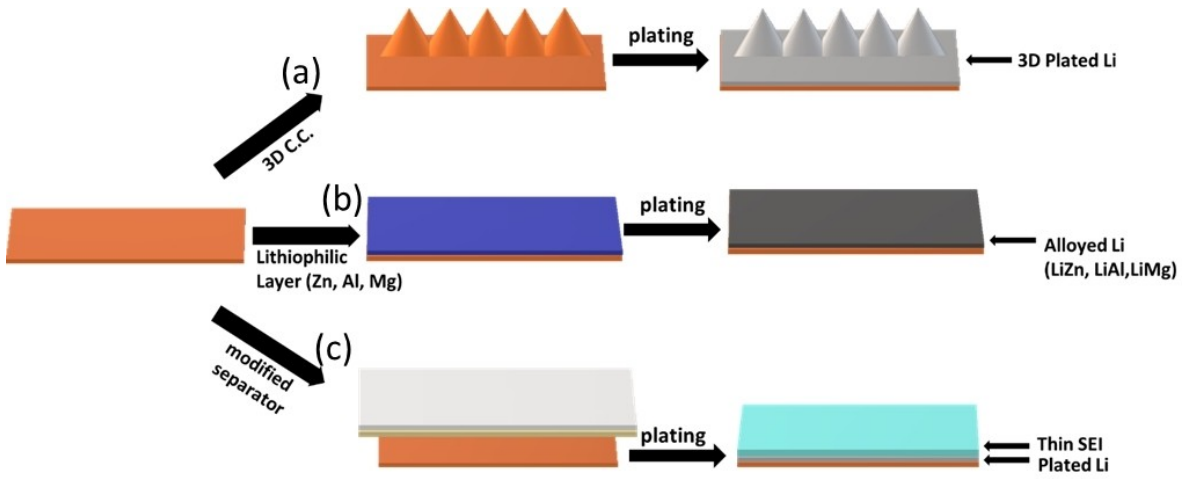

Figure 7. Schematic representing the possible modification methods of a CC.

preferentially formed compared to lithium deposition on the Cu substrate. Using an Ag layer over Cu can increase the discharge capacity toward $LiFePO_4$ cathode by approximately 20% throughout the cycles. Tang et al.[103] developed a polypropylene (PP) separator coated with polydopamine (PDA) and aluminum nitride (AlN), which promoted uniform Li^+ flux and reduced the migration barrier for dendrite-free lithium deposition. The PDA@AlN@PP separator showed excellent electrolyte wettability, mechanical performance, and thermal resistance, and it served as a robust barrier against dendrite penetration and reduced the dead lithium formation. Song et al.[104] employed Mo-containing polyoxometalates (POM) modified separators in the LMBs to inhibit the formation of lithium dendrites. When lithium dendrites touch the separator, an optimized POM oxidizes dead lithium into Li^+ ions, which are released into the cell system to participate in subsequent electrochemical cycles and stabling cycle life. A 3D protective layer (consisting of $ZnCl_2$ and PVDF) on the lithium anode has been developed via electrospinning for LMB application.[105] It enhances lithium deposition, wettability, and Li^+ flux, and reduces interface resistance. Chemical anchoring of $ZnCl_2$ on the PVDF framework induces super-lithiophilicity to digest Li dendrites, resulted in minimizing dead lithium. Wang et al.[106] developed a method to form a novel hydrogen-bond-induced strategy on PVDF coatings with improved ferroelectric polarization for LMBs (Figure 7c). The PVDF coating has neatly arranged dipoles that provide an internal electric field and effectively reduces lithium dendrite growth and dead lithium formation. As a result, this technique enables the high-rate capability of designed cells. Zhang et al.[107] have modified the CC by using a mixture of polymetylmetacrilate (PMMA) and yttrium trifluoride YF_3. A dense lithium deposition can be obtained through a Y-doped (200) crystal plane which promotes the transformation of the preferred oriented growth to (200) crystal plane from (110) plane by reducing the possible side reactions related to the contact with the electrolyte.

Sun et al.[90] utilized an artificial-SEI on a Cu CC that combined lithium fluoride and lithium phosphorus oxynitride (LiF–LiPON/Cu) to achieve improved ionic conductivity (10^{-6} S cm^{-1}) and durability. The artificial-SEI film can somewhat inhibit the unrestricted growth of lithium dendrites because of its uniform ion transport and high Young's modulus. Using the LiF–LiPON/Cu electrodes reduced the amount of dead lithium compared to using bare Cu CC electrodes. The modification of current collector may increase the battery fabrication costs, especially if physical deposition techniques are used to prepare thin films.

3.3. Use of Solid-State Electrolytes

The formation of dead lithium can be facilitated by using an electrolyte with a low transference number. As for example, the use of Polyethylene Oxide (PEO)-LiTFSI as solid electrolyte in Cu//LiFePO4 cell exhibits a poor cyclability as shown by Bertoli et al. The addition of Zn terephthalate could increase the first discharge capacity (120 mAh g^{-1} vs 40 mAh g^{-1}) while the cycle life didn't improve.[108] Wang et al.[109] have created a stable anode-free all-solid-state battery using sulfide-based solid-electrolyte material. A Li_2Te coating of 1 μm thickness on Cu CC reduces plating/stripping overpotentials and improves CE. The coated Cu CC promotes homogeneous lithium plating, a thin and uniform SEI layer, and the forming of inactive dead metal during cycling is greatly avoided. Undesired chemical reactions between the electrolyte and electrode materials, such as lithium plating/stripping, can consume Li-ions irreversibly and produce dead lithium. As reported by Zhang et al.[110] pores and cracks may be induced by particle size randomness which can facilitate the propagation of dendrites. On the contrary using cube-shaped argyrodite can be able to better densify the pellet reducing the porosity. Reactivating dead lithium is a promising approach to slow down lithium consumption and enhance interface stability. A homogenous Li^+ ions distribution can reduce the possibility to create dendrites and dead lithium by using a solid electrolyte. If ceramic is not perfectly dense, possibly lithium can penetrate through the grain boundaries or

accumulate where voids are present.[111,112] The company Quantumscape[113] was able to limit the formation of dead lithium by using an ultra-dense garnet-based solid electrolyte. As weakness, ceramic electrolytes are much more expensive than liquid electrolytes although their high transference number make them suitable to develop efficient AFLMBs.

Table 1 summarizes the key performance metrics, advantages, and challenges associated with different mitigation strategies. As shown in the table, each strategy presents a unique set of trade-offs, and the optimal choice will depend on the specific requirements of the battery application.

4. Conclusions, Perspectives and Outlook

4.1. Conclusions

LMBs and AFLMBs hold immense potential due to their high energy densities. However, a critical challenge hindering their practical application is the formation of "dead lithium." These are electrochemically inactive lithium fragments that accumulate during battery cycling. Dead lithium reduces battery capacity and lifespan, increases internal resistance leading to heat generation, and promotes the growth of lithium dendrites, posing safety risks. Understanding the factors that influence dead lithium formation is crucial for developing mitigation strategies. Slower lithium stripping at higher temperatures and currents, thin and narrow electrode interfaces, and electrolyte compositions that hinder diffusion processes can all contribute to dead lithium formation. The SEI can also play a double-edged role on dead lithium formation. While essential for preventing unwanted reactions, a thick or poorly conductive SEI can trap lithium ions, reducing their reversibility and contributing to dead lithium formation.

Additionally, the morphology of lithium plating itself matters on dead lithium formation. Dendritic lithium deposits, with their high surface area and uneven distribution, are more prone to dead lithium formation compared to smooth morphologies.

Researchers are actively exploring various strategies to combat dead lithium formation. Optimizing electrolyte chemistry is a key area of focus. Additives like FEC have been shown to suppress dead lithium formation, while electrolytes that promote fast and homogeneous SEI formation can also be beneficial. Artificial SEI layers with improved stability and conductivity offer another promising approach. Techniques to reactivate dead lithium, like using redox mediators are also being explored. Modifying the CC could play a vital role as well, although the high costs related to the manufacturing process may limit the technique. 3D CCs can promote uniform lithium deposition, while lithiophilic layers can encourage homogenous plating. Modified separators that oxidize dead lithium are further strategies. Finally, solid-state electrolytes with high lithium-ion mobility hold promise for minimizing dead lithium formation by ensuring homogenous Li^+ distribution. By implementing these diverse strategies that target electrolyte chemistry, SEI properties, electrode design, and CC modification, researchers are making significant strides towards mitigating dead lithium formation and unlocking the full potential of LMBs and AFLMBs for next-generation energy storage solutions. New liquid electrolytes should be designed to reduce the possible side reactions with plated lithium metal. The preparation of a full ceramic AFLMB is limited by the high costs of fabrication and the presence of residual porosity which cannot block lithium dendrites propagation. New ceramic-polymer composite should be prepared considering the use of additives such as lithiophilic agent (e.g a Zn-based salt) or protective layer (e.g Lithium borate-based salt).

Based on our discussions and analysis, the following strategies appear particularly promising for enhancing the interface where lithium plating and stripping occur:

4.1.1. Electrolyte Engineering

Developing novel electrolyte formulations with additives can suppress dead lithium formation and promote the formation of a stable SEI. Solid-state electrolytes offer intrinsic safety benefits and can further mitigate dendrite formation.

4.1.2. Electrode Design

Utilizing current collectors with lithiophilic coatings can facilitate uniform lithium deposition, thereby reducing dendrite growth and dead lithium formation.

In conclusion, dead lithium probably represents the biggest challenge in the development and deployment of AFLMBs, impacting their capacity, efficiency, and safety. However, through interdisciplinary research efforts spanning materials science, electrochemistry, battery diagnostics, artificial intelligence (AI), and battery management systems (BMS) innovative solutions are being developed to mitigate the effects of dead lithium and unlock the full potential of lithium battery technology. By addressing this challenge, we can accelerate the transition towards a sustainable and electrified future, powering the global transition to renewable energy and decarbonizing transportation.

4.2. Perspectives

- The formation and evolution of dead lithium is not a static event but a dynamic process influenced by various factors throughout the battery's lifecycle. Understanding this dynamic nature can lead to more effective mitigation strategies that adapt to changing battery conditions.
- While dendrite growth is a major contributor to dead lithium formation, other factors such as SEI properties, electrolyte composition, and electrode morphology also play significant roles. A holistic approach considering all these factors is necessary for comprehensive mitigation.
- Instead of just preventing dead lithium formation, exploring ways to reactivate or recycle dead lithium could offer a new

Table 1. Performance comparison of AFLMBs with different mitigation strategies.*

Mitigation Strategy	Key Performance Metrics	Advantages	Challenges
Electrolyte Additives	Improved Coulombic Efficiency (CE) Reduced dead lithium formation Enhanced capacity retention	Simple implementation Low cost	Additive degradation over time Limited effectiveness at high currents
3D Current Collectors	Uniform lithium deposition Reduced dendrite growth and dead lithium Improved rate capability	Enhanced safety Increased lifespan	Increased complexity and cost Potential for higher surface area leading to increased SEI formation
Lithiophilic Coatings on Current Collectors	Homogeneous lithium plating Reduced dendrite growth and dead lithium Improved cycle life	Relatively simple implementation Can be combined with other strategies	Potential for coating degradation Limited effectiveness at high currents
Modified Separators	Uniform Li^+ flux Reduced dendrite penetration Improved safety	Can incorporate multiple functionalities (e.g., $LiNO_3$ release, dendrite oxidation)	Potential for separator degradation May increase cell thickness and resistance
Solid-State Electrolytes	High Li^+ conductivity Dendrite suppression Enhanced safety	Potential for high energy density with Li metal anodes Improved stability at high voltages	High interfacial resistance Challenges in manufacturing and scalability High cost
Artificial SEI Layers	Improved interfacial stability Reduced dendrite growth and dead lithium Enhanced cycle life	Can be tailored for specific properties (e.g., ionic conductivity, mechanical strength) Can be combined with other strategies	Challenges in uniform deposition and scalability Potential for long-term stability issues
Reactivation of Dead Lithium (e.g., Redox Mediators)	Recovery of inactive lithium Improved capacity retention Extended cycle life	Innovative approach to address dead lithium Can be combined with other strategies	Complexity of redox mediator design and implementation Potential for side reactions and self-discharge

* The specific performance metrics and advantages/challenges can vary depending on the specific materials and implementation details of each strategy. The table provides a general overview based on the information presented in this manuscript, which is obtained from many references. It's important to critically evaluate the performance of different strategies under various conditions (e.g., current densities, temperatures, cycle life) to determine their suitability for specific AFLMB applications.

avenue for improving battery performance and resource efficiency. This could involve developing novel electrolyte additives or electrode designs that facilitate the reintegration of dead lithium into the electrochemical cycle.
- Dead lithium formation occurs at multiple scales, from the nanoscale SEI layer to the macroscale electrode structure. A multi-scale understanding, combining experimental observations with computational modeling, is crucial for unraveling the complex mechanisms and developing targeted mitigation strategies.
- The increasing availability of data from advanced characterization techniques and battery management systems opens up opportunities for data-driven approaches to dead lithium mitigation. Machine learning algorithms could be used to predict dead lithium formation based on real-time battery data, enabling proactive interventions to improve battery performance and safety.

4.3. Outlook

- Continued development of advanced characterization techniques, such as in situ/operando microscopy and spectroscopy, will provide deeper insights into the dynamic processes of dead lithium formation, enabling researchers to design more effective mitigation strategies.
- Artificial intelligence (AI) and machine learning can play a crucial role in accelerating the development of new materials and electrolytes for mitigating dead lithium formation. These tools can be used to analyze large datasets, identify patterns, and predict the performance of new materials, leading to faster and more efficient material discovery.
- While the focus is currently on lithium-based batteries, the insights gained from dead lithium research can be extended to other next-generation battery technologies, such as sodium- and magnesium-metal batteries, which may also face similar challenges. However, we are also actively investigating the formation and mitigation strategies of dead metals beyond lithium, which will be the subject of our forthcoming publication.
- Developing strategies to reactivate dead lithium aligns with the principles of sustainability and circular economy. By reducing waste and maximizing resource utilization, we can create a more sustainable and environmentally friendly battery industry.

Author Contributions

Both authors contributed equally to this paper.

Acknowledgements

This work was supported by the financial support of the German Federal Ministry for Education and Research (BMBF) for the funding of the research project of SiLiNE (Reference No. 03XP0419B). Open Access funding enabled and organized by Projekt DEAL.

Conflict of Interests

The authors declare no conflict of interest.

Data Availability Statement

Data sharing is not applicable to this article as no new data were created or analyzed in this study.

Keywords: Dead lithium formation · Anode-free batteries · Lithium-metal batteries · Mitigation strategies

[1] C. Fang, J. Li, M. Zhang, Y. Zhang, F. Yang, J. Z. Lee, M.-H. Lee, J. Alvarado, M. A. Schroeder, Y. Yang, *Nature* **2019**, *572*, 511–515.
[2] P. G. Bruce, S. A. Freunberger, L. J. Hardwick, J.-M. Tarascon, *Nat. Mater.* **2012**, *11*, 19–29.
[3] Z. Liu, M. Chen, D. Zhou, Z. Xiao, *Adv. Funct. Mater.* **2023**, *33*, 2306321.
[4] D. Petersen, M. Gronenberg, G. Lener, E. Leiva, G. L. Luque, S. Rostami, A. Paolella, B. J. Hwang, R. Adelung, M. Abdollahifar, *Mater. Horiz.* **2024**.
[5] P. Albertus, S. Babinec, S. Litzelman, A. Newman, *Nat. Energy* **2018**, *3*, 16–21, https://doi.org/10.1038/s41560-017-0047-2.
[6] Z. Zhao, X. Zhao, Y. Zhou, S. Liu, G. Fang, S. Liang, *Adv. Powder Mater.* **2023**, *2*, 100139, https://doi.org/10.1016/j.apmate.2023.100139.
[7] P. Molaiyan, M. Abdollahifar, B. Boz, A. Beutl, M. Krammer, N. Zhang, A. Tron, M. Romio, M. Ricci, R. Adelung, *Adv. Funct. Mater.* **2024**, *34*, 2311301.
[8] X. Shen, Y. Li, T. Qian, J. Liu, J. Zhou, C. Yan, J. B. Goodenough, *Nat. Commun.* **2019**, *10*, 900. https://doi.org/10.1038/s41467-019-08767-0.
[9] H. Cavers, P. Molaiyan, M. Abdollahifar, U. Lassi, A. Kwade, *Adv. Energy Mater.* **2022**, *12*, 2200147.
[10] S. Nanda, A. Gupta, A. Manthiram, *Adv. Energy Mater.* **2021**, *11*, 2000804. https://doi.org/10.1002/aenm.202000804.
[11] Y. Chen, M. Yue, C. Liu, H. Zhang, Y. Yu, X. Li, H. Zhang, *Adv. Funct. Mater.* **2019**, *29*, 1806752, https://doi.org/10.1002/adfm.201806752.
[12] J. Liu, T. Qian, N. Xu, M. Wang, J. Zhou, X. Shen, C. Yan, *Energy Storage Mater.* **2020**, *24*, 265–271, https://doi.org/10.1016/j.ensm.2019.08.010.
[13] D.-H. Liu, Z. Bai, M. Li, A. Yu, D. Luo, W. Liu, L. Yang, J. Lu, K. Amine, Z. Chen, *Chem. Soc. Rev.* **2020**, *49*, 5407–5445.
[14] C. Fang, X. Wang, Y. S. Meng, *Trends Chem.* **2019**, *1*, 152–158.
[15] H. Chen, J. Liu, X. Zhou, H. Ji, S. Liu, M. Wang, T. Qian, C. Yan, *Chem. Eng. J.* **2021**, *404*, 126470, https://doi.org/10.1016/j.cej.2020.126470.
[16] Y. Zhao, Y. Wu, H. Liu, S.-L. Chen, S.-H. Bo, *ACS Appl. Mater. Interfaces* **2021**, *13*, 35750–35758.
[17] G. Yoon, S. Moon, G. Ceder, K. Kang, *Chem. Mater.* **2018**, *30*, 6769–6776.
[18] X. Shen, R. Zhang, P. Shi, X.-Q. Zhang, X. Chen, C.-Z. Zhao, P. Wu, Y.-M. Guo, J.-Q. Huang, Q. Zhang, *Fundam. Res.* **2022**.
[19] R. Zhang, X. Shen, Y.-T. Zhang, X.-L. Zhong, H.-T. Ju, T.-X. Huang, X. Chen, J.-D. Zhang, J.-Q. Huang, *J. Energy Chem.* **2022**, *71*, 29–35.
[20] D. Tewari, S. P. Rangarajan, P. B. Balbuena, Y. Barsukov, P. P. Mukherjee, *J. Phys. Chem. C* **2020**, *124*, 6502–6511.
[21] H. G. Lee, S. Y. Kim, J. S. Lee, *npj Comput. Mater.* **2022**, *8*, 103, https://doi.org/10.1038/s41524-022-00788-6.
[22] D. Tewari, P. P. Mukherjee, *J. Mater. Chem. A* **2019**, *7*, 4668–4688.
[23] S. Zhang, J.-F. Ding, R. Xu, Y. Xiao, C. Yan, J.-Q. Huang, *Adv. Energy Mater.* **2024**, *14*, 2303726.
[24] A. J. Sanchez, E. Kazyak, Y. Chen, K.-H. Chen, E. R. Pattison, N. P. Dasgupta, *ACS Energy Lett.* **2020**, *5*, 994–1004.
[25] A. J. Sanchez, N. P. Dasgupta, *J. Am. Chem. Soc.* **2024**, *146*, 4282–4300.
[26] M. Tao, X. Chen, H. Lin, Y. Jin, P. Shan, D. Zhao, M. Gao, Z. Liang, Y. Yang, *ACS Nano* **2023**, *17*, 24104–24114.
[27] H. Lee, X. Ren, C. Niu, L. Yu, M. H. Engelhard, I. Cho, M.-H. Ryou, H. S. Jin, H.-T. Kim, J. Liu, *Adv. Funct. Mater.* **2017**, *27*, 1704391.
[28] X.-R. Chen, B.-C. Zhao, C. Yan, Q. Zhang, *Adv. Mater.* **2021**, *33*, 2004128.

[29] D. T. Boyle, S. C. Kim, S. T. Oyakhire, R. A. Vilá, Z. Huang, P. Sayavong, J. Qin, Z. Bao, Y. Cui, *J. Am. Chem. Soc.* **2022**, *144*, 20717–20725.
[30] Y.-X. Zhan, P. Shi, X.-X. Ma, C.-B. Jin, Q.-K. Zhang, S.-J. Yang, B.-Q. Li, X.-Q. Zhang, J.-Q. Huang, *Adv. Energy Mater.* **2022**, *12*, 2103291.
[31] K. S. Vikrant, E. McShane, A. M. Colclasure, B. D. McCloskey, S. Allu, *J. Electrochem. Soc.* **2022**, *169*, 40520.
[32] C. Liu, Z. Cui, A. Manthiram, *Adv. Energy Mater.* **2024**, *14*, 2302722.
[33] X. Duan, B. Li, J. Li, X. Gao, L. Wang, J. Xu, *Adv. Energy Mater.* **2023**, *13*, 2203767.
[34] W. Zhu, H. Demers, G. Girard, D. Clement, F. Zimin, A. Guerfi, M. Trudeau, A. Vijh, A. Paolella, *J. Power Sources* **2022**, *546*, 231941, https://doi.org/10.1016/j.jpowsour.2022.231941.
[35] J. Liu, Z. Bao, Y. Cui, E. J. Dufek, J. B. Goodenough, P. Khalifah, Q. Li, B. Y. Liaw, P. Liu, A. Manthiram, *Nat. Energy* **2019**, *4*, 180–186.
[36] D. Lu, Y. Shao, T. Lozano, W. D. Bennett, G. L. Graff, B. Polzin, J. Zhang, M. H. Engelhard, N. T. Saenz, W. A. Henderson, *Adv. Energy Mater.* **2015**, *5*, 1400993.
[37] B. L. Mehdi, J. Qian, E. Nasybulin, C. Park, D. A. Welch, R. Faller, H. Mehta, W. A. Henderson, W. Xu, C. M. Wang, *Nano Lett.* **2015**, *15*, 2168–2173.
[38] P. Bai, J. Li, F. R. Brushett, M. Z. Bazant, *Energy Environ. Sci.* **2016**, *9*, 3221–3229.
[39] S.-Y. Lee, J. Shangguan, S. Betzler, S. J. Harris, M. M. Doeff, H. Zheng, *Nano Energy* **2022**, *102*, 107641, https://doi.org/10.1016/j.nanoen.2022.107641.
[40] K.-H. Chen, K. N. Wood, E. Kazyak, W. S. LePage, A. L. Davis, A. J. Sanchez, N. P. Dasgupta, *J. Mater. Chem. A* **2017**, *5*, 11671–11681.
[41] S. Xu, K.-H. Chen, N. P. Dasgupta, J. B. Siegel, A. G. Stefanopoulou, *J. Electrochem. Soc.* **2019**, *166*, A3456–A3463.
[42] M. Romio, J. Kahr, E. Miele, M. Krammer, Y. Surace, B. Boz, P. Molaiyan, T. Dimopoulos, M. Armand, A. Paolella, *Adv. Mater. Technol.* **2024**, 2301902, https://doi.org/10.1002/admt.202301902.
[43] K. J. Harry, D. T. Hallinan, D. Y. Parkinson, A. A. MacDowell, N. P. Balsara, *Nat. Mater.* **2014**, *13*, 69–73.
[44] S. Chandrashekar, N. M. Trease, H. J. Chang, L.-S. Du, C. P. Grey, A. Jerschow, *Nat. Mater.* **2012**, *11*, 311–315.
[45] X. Wang, M. Zhang, J. Alvarado, S. Wang, M. Sina, B. Lu, J. Bouwer, W. Xu, J. Xiao, J.-G. Zhang, *Nano Lett.* **2017**, *17*, 7606–7612.
[46] X. Zhang, Z. Guo, X. Li, Q. Liu, H. Hu, F. Li, Q. Huang, L. Zhang, Y. Tang, J. Huang, *Energy Environ. Sci.* **2024**, *17*.
[47] C. Xu, B. Sun, T. Gustafsson, K. Edström, D. Brandell, M. Hahlin, *J. Mater. Chem. A* **2014**, *2*, 7256–7264.
[48] M. J. Zachman, Z. Tu, S. Choudhury, L. A. Archer, L. F. Kourkoutis, *Nature* **2018**, *560*, 345–349.
[49] Y.-C. Hsieh, M. Leißing, S. Nowak, B.-J. Hwang, M. Winter, G. Brunklaus, *Cell Rep. Phys. Sci.* **2020**, *1*, 100139.
[50] A. B. Gunnarsdóttir, C. V. Amanchukwu, S. Menkin, C. P. Grey, *J. Am. Chem. Soc.* **2020**, *142*, 20814–20827.
[51] Z. Liang, Y. Xiang, K. Wang, J. Zhu, Y. Jin, H. Wang, B. Zheng, Z. Chen, M. Tao, X. Liu, *Nat. Commun.* **2023**, *14*, 259.
[52] Q. Wang, C. Zhao, J. Wang, Z. Yao, S. Wang, S. G. H. Kumar, S. Ganapathy, S. Eustace, X. Bai, B. Li, *Nat. Commun.* **2023**, *14*, 440.
[53] A. J. Smith, Y. Fang, A. Mikheenkova, H. Ekström, P. Svens, I. Ahmed, M. J. Lacey, G. Lindbergh, I. Furó, R. W. Lindström, *J. Power Sources* **2023**, *573*, 233118, https://doi.org/10.1016/j.jpowsour.2023.233118.
[54] A. B. Gunnarsdóttir, S. Vema, S. Menkin, L. E. Marbella, C. P. Grey, *J. Mater. Chem. A* **2020**, *8*, 14975–14992.
[55] R. Bhattacharyya, B. Key, H. Chen, A. S. Best, A. F. Hollenkamp, C. P. Grey, *Nat. Mater.* **2010**, *9*, 504–510.
[56] X. Shen, R. Zhang, P. Shi, X. Chen, Q. Zhang, *Adv. Energy Mater.* **2021**, *11*, 2003416.
[57] C. Fang, B. Lu, G. Pawar, M. Zhang, D. Cheng, S. Chen, M. Ceja, J.-M. Doux, H. Musrock, M. Cai, *Nat. Energy* **2021**, *6*, 987–994.
[58] X. Lin, Y. Shen, Y. Yu, Y. Huang, *Adv. Energy Mater.* **2024**, *14*, 2303918.
[59] N. R. Geise, R. M. Kasse, J. Nelson Weker, H.-G. Steinrück, M. F. Toney, *Chem. Mater.* **2021**, *33*, 7537–7545, https://doi.org/10.1021/acs.chemmater.1c02585.
[60] C. Gervillié-Mouravieff, L. Ah, A. Liu, C.-J. Huang, Y. S. Meng, *ACS Energy Lett.* **2024**, *9*, 1693–1700.
[61] J.-F. Ding, R. Xu, Y. Xiao, S. Zhang, T.-L. Song, C. Yan, J.-Q. Huang, *Adv. Energy Mater.* **2023**, *13*, 2204305.
[62] H. Gao, Q. Yan, J. Holoubek, Y. Yin, W. Bao, H. Liu, A. Baskin, M. Li, G. Cai, W. Li, *Adv. Energy Mater.* **2023**, *13*, 2202906.
[63] H. Shen, P. Tang, Q. Wei, Y. Zhang, T. Yu, H. Yang, R. Zhang, K. Tai, J. Tan, S. Bai, F. Li, *Small* **2023**, *19*, 2206000, https://doi.org/10.1002/smll.202206000.
[64] Y. Xie, Y. Huang, H. Chen, W. Lin, T. Wu, Y. Wang, S. Liu, M. Sun, H. Huang, P. Dai, *Adv. Funct. Mater.* **2024**, *34*, 2310867.
[65] Y. Xie, Y. Huang, Y. Zhang, T. Wu, S. Liu, M. Sun, B. Lee, Z. Lin, H. Chen, P. Dai, *Nat. Commun.* **2023**, *14*, 2883.
[66] Z. M. Konz, B. M. Wirtz, A. Verma, T.-Y. Huang, H. K. Bergstrom, M. J. Crafton, D. E. Brown, E. J. McShane, A. M. Colclasure, B. D. McCloskey, *Nat. Energy* **2023**, *8*, 450–461.
[67] M. Tao, Y. Xiang, D. Zhao, P. Shan, Y. Sun, Y. Yang, *Nano Lett.* **2022**, *22*, 6775–6781.
[68] P. Daubinger, M. Göttlinger, S. Hartmann, G. A. Giffin, *Batteries Supercaps* **2023**, *6*, e202200452.
[69] Y. Xiang, M. Tao, X. Chen, P. Shan, D. Zhao, J. Wu, M. Lin, X. Liu, H. He, W. Zhao, *Nat. Commun.* **2023**, *14*, 177.
[70] R. A. Vilá, D. T. Boyle, A. Dai, W. Zhang, P. Sayavong, Y. Ye, Y. Yang, J. A. Dionne, Y. Cui, *Sci. Adv.* **2023**, *9*, eadf3609.
[71] R. Schmitz, R. Müller, S. Krüger, R. W. Schmitz, S. Nowak, S. Passerini, M. Winter, C. Schreiner, *J. Power Sources* **2012**, *217*, 98–101, https://doi.org/10.1016/j.jpowsour.2012.05.038.
[72] M. Golozar, P. Hovington, A. Paolella, S. Bessette, M. Lagacé, P. Bouchard, H. Demers, R. Gauvin, K. Zaghib, *Nano Lett.* **2018**, *18*, 7583–7589, https://doi.org/10.1021/acs.nanolett.8b03148.
[73] M. Golozar, A. Paolella, H. Demers, S. Savoie, G. Girard, N. Delaporte, R. Gauvin, A. Guerfi, H. Lorrmann, K. Zaghib, *Sci. Rep.* **2020**, *10*, 18410.
[74] Y. Xiang, M. Tao, G. Zhong, Z. Liang, G. Zheng, X. Huang, X. Liu, Y. Jin, N. Xu, M. Armand, *Sci. Adv.* **2021**, *7*, eabj3423.
[75] S. Ni, M. Zhang, C. Li, R. Gao, J. Sheng, X. Wu, G. Zhou, *Adv. Mater.* **2023**, *35*, 2209028.
[76] G. Peng, Q. Zheng, G. Luo, D. Zheng, S.-P. Feng, U. Khan, A. R. Akbar, H. Luo, F. Liu, *Small* **2023**, *19*, 2303787.
[77] C. Chang, M. Zhang, Z. Lao, X. Xiao, G. Lu, H. Qu, X. Wu, H. Fu, G. Zhou, *Adv. Mater.* **2024**, *36*, 2313525.
[78] Z. Yu, H. Wang, X. Kong, W. Huang, Y. Tsao, D. G. Mackanic, K. Wang, X. Wang, W. Huang, S. Choudhury, *Nat. Energy* **2020**, *5*, 526–533.
[79] C. Jin, T. Liu, O. Sheng, M. Li, T. Liu, Y. Yuan, J. Nai, Z. Ju, W. Zhang, Y. Liu, *Nat. Energy* **2021**, *6*, 378–387.
[80] Q. Wang, C. Zhao, Z. Yao, J. Wang, F. Wu, S. G. H. Kumar, S. Ganapathy, S. Eustace, X. Bai, B. Li, *Adv. Mater.* **2023**, *35*, 2210677.
[81] Y. Chen, M. Li, Y. Liu, Y. Jie, W. Li, F. Huang, X. Li, Z. He, X. Ren, Y. Chen, *Nat. Commun.* **2023**, *14*, 2655.
[82] Y. Gao, Z. Yan, J. L. Gray, X. He, D. Wang, T. Chen, Q. Huang, Y. C. Li, H. Wang, S. H. Kim, *Nat. Mater.* **2019**, *18*, 384–389.
[83] M. Mao, X. Ji, Q. Wang, Z. Lin, M. Li, T. Liu, C. Wang, Y.-S. Hu, H. Li, X. Huang, *Nat. Commun.* **2023**, *14*, 1082.
[84] J. A. Weeks, J. N. Burrow, J. Diao, A. G. Paul-Orecchio, H. S. Srinivasan, R. R. Vaidyula, A. Dolocan, G. Henkelman, C. B. Mullins, *Adv. Mater.* **2023**, *36*, 2305645.
[85] D. Lin, Y. Liu, Z. Liang, H.-W. Lee, J. Sun, H. Wang, K. Yan, J. Xie, Y. Cui, *Nat. Nanotechnol.* **2016**, *11*, 626–632.
[86] H. Chen, A. Pei, J. Wan, D. Lin, R. Vilá, H. Wang, D. Mackanic, H.-G. Steinrück, W. Huang, Y. Li, *Joule* **2020**, *4*, 938–952.
[87] Z. Zhu, X. Li, X. Qi, J. Ji, Y. Ji, R. Jiang, C. Liang, D. Yang, Z. Yang, L. Qie, *Nano-Micro Lett.* **2023**, *15*, 234.
[88] T. Naren, R. Jiang, P. Qing, S. Huang, C. Ling, J. Lin, W. Wei, X. Ji, Y. Chen, Q. Zhang, *ACS Nano* **2023**, *17*, 20315–20324.
[89] C. Guo, Z.-H. Luo, M.-X. Zhou, X. Wu, Y. Shi, Q. An, J.-J. Shao, G. Zhou, *Small* **2023**, *19*, 2301428.
[90] J. Sun, S. Zhang, J. Li, B. Xie, J. Ma, S. Dong, G. Cui, *Adv. Mater.* **2023**, *35*, 2209404.
[91] Q. Dong, M. Wang, X. Huang, B. Hong, Y. Lai, *ACS Appl. Mater. Interfaces* **2023**, *15*, 17386–17395, https://doi.org/10.1021/acsami.3c01266.
[92] M. Yeddala, L. Rynearson, B. L. Lucht, *ACS Energy Lett.* **2023**, *8*, 4782–4793, https://doi.org/10.1021/acsenergylett.3c01709.
[93] E. Zhang, H. Tian, M. Li, S. Le, B. Li, L. Wu, Q. Zhang, L. Fan, *Chem. Commun.* **2023**, *59*, 10996–10999.
[94] S. Stuckenberg, M. M. Bela, C.-T. Lechtenfeld, M. Mense, V. Küpers, T. T. K. Ingber, M. Winter, M. C. Stan, *Small* **2024**, *20*, 2305203.
[95] J. Chen, Z. Cheng, Y. Liao, L. Yuan, Z. Li, Y. Huang, *Adv. Energy Mater.* **2022**, *12*, 2201800.
[96] C.-B. Jin, X.-Q. Zhang, O.-W. Sheng, S.-Y. Sun, L.-P. Hou, P. Shi, B.-Q. Li, J.-Q. Huang, X.-Y. Tao, Q. Zhang, *Angew. Chem. Int. Ed.* **2021**, *60*, 22990–22995, https://doi.org/10.1002/anie.202110589.

[97] Q. Li, H. Liu, F. Wu, L. Li, Y. Ye, R. Chen, *Angew. Chem. Int. Ed.* **2024**, *63*, e202404554, https://doi.org/10.1002/anie.202404554.
[98] Q. Li, H. Liu, F. Wu, L. Li, Y. Ye, R. Chen, *Angew. Chem. Int. Ed.* **2024**, *63*, e202404554.
[99] Y. Zhou, X. Zhang, Y. Ding, L. Zhang, G. Yu, *Adv. Mater.* **2020**, *32*, 2005763. https://doi.org/10.1002/adma.202005763.
[100] P. Qing, Z. Wu, A. Wang, S. Huang, K. Long, T. Naren, D. Chen, P. He, H. Huang, Y. Chen, *Adv. Mater.* **2023**, *35*, 2211203.
[101] P. Afzali, E. Gibertini, L. Magagnin, *Electrochim. Acta* **2024**, *488*, 144190.
[102] W. Shin, A. Manthiram, *ACS Appl. Mater. Interfaces* **2022**, *14*, 17454–17460.
[103] W. Tang, T. Zhao, K. Wang, T. Yu, R. Lv, L. Li, F. Wu, R. Chen, *Adv. Funct. Mater.* **2024**, *34*, 2314045.
[104] J. Song, Y. Jiang, Y. Lu, Y. Cao, Y. Zhang, L. Fan, H. Liu, G. Gao, *Small* **2023**, *19*, 2301740.
[105] Y. Hu, Z. Li, Z. Wang, X. Wang, W. Chen, J. Wang, W. Zhong, R. Ma, *Adv. Sci.* **2023**, *10*, 2206995.
[106] W. Wang, L. Ma, B. Xu, H. Zhu, C. Zhang, L. Chen, W. Wei, *Small* **2024**, *20*, 2305797.
[107] Y. Zhang, R. Qiao, Q. Nie, P. Zhao, Y. Li, Y. Hong, S. Chen, C. Li, B. Sun, H. Fan, *Nat. Commun.* **2024**, *15*, 4454.
[108] L. Bertoli, S. Bloch, E. Andersson, L. Magagnin, D. Brandell, J. Mindemark, *Electrochim. Acta* **2023**, *464*, 142874, https://doi.org/10.1016/j.electacta.2023.142874.
[109] Y. Wang, Y. Liu, M. Nguyen, J. Cho, N. Katyal, B. S. Vishnugopi, H. Hao, R. Fang, N. Wu, P. Liu, *Adv. Mater.* **2023**, *35*, 2206762.
[110] X. Zhang, M. Zhang, J. Wu, X. Hu, B. Fu, Z. Zhang, B. Luo, K. Khan, Z. Fang, Z. Xu, *Nano Energy* **2023**, *115*, 108700.
[111] H. Sun, Q. Liu, J. Chen, Y. Li, H. Ye, J. Zhao, L. Geng, Q. Dai, T. Yang, H. Li, *ACS Nano* **2021**, *15*, 19070–19079.
[112] Y. Liu, H. Su, Y. Zhong, M. Zheng, Y. Hu, F. Zhao, J. T. Kim, Y. Gao, J. Luo, X. Lin, J. Tu, X. Sun, *Adv. Energy Mater.* **2024**, 2400783, https://doi.org/10.1002/aenm.202400783.
[113] C.-C. Chao, L. Cheng, C. Dekmezian, T. Ho, T. Holme, T. Huang, A. Mehrotra, A. Yang, Quantumscape Corporation, PCT/US2018/059505, **2019**.

Manuscript received: July 26, 2024
Revised manuscript received: September 23, 2024
Accepted manuscript online: September 26, 2024
Version of record online: November 4, 2024